The Journal of Molecular Diagnostics, Vol. 22, No. 5, May 2020

ELSEVIER

the Journal of Molecular Diagnostics
jmd.amjpathol.org

Immune Profiling of Deficient Mismatch Repair Colorectal Cancer Tumor Microenvironment Reveals Different Levels of Immune System Activation

Riccardo Giannini,* Gemma Zucchelli,† Mirella Giordano,* Clara Ugolini,‡ Roberto Moretto,† Katarzyna Ambryszewska,§ Michele Leonardi,§ Elisa Sensi,‡ Federica Morano,¶ Filippo Pietrantonio,¶‖ Chiara Cremolini,† Alfredo Falcone,† and Gabriella Fontanini*

From the Departments of Surgical, Medical and Molecular Pathology and Critical Care Medicine and Pharmacy,§ University of Pisa, Pisa; the Unit of Medical Oncology,† Azienda Ospedaliero—Universitaria Pisana, Department of Translational Research and New Technologies in Medicine, University of Pisa, Pisa; the Unit of Anatomic Pathology 3,‡ Azienda Ospedaliero—Universitaria Pisana, Pisa; the Medical Oncology Department,¶ Fondazione Istituti di Ricovero e Cura a Carattere Scientifico Istituto Nazionale dei Tumori di Milano,‖ University of Milan, Milan, Italy*

Accepted for publication February 10, 2020.

Address correspondence to Gabriella Fontanini, M.D., Ph.D., Department of Surgical, Medical and Molecular Pathology and Critical Care Medicine, University of Pisa, 57 Via Roma, I-56126 Pisa, Italy. E-mail: gabriella.fontanini@med.unipi.it.

To understand the immune landscape of deficient mismatch repair colorectal cancer (dMMR CRC) tumor microenvironment, gene expression profiling was performed by the nCounter PanCancer Immune Profiling Panel. This study was conducted retrospectively on 89 dMMR-CRC samples. The expression of CD3, CD8, programmed death-1, and programmed death ligand-1 protein was evaluated on a subset of samples by immunohistochemistry, and lymphocyte density was calculated. A subset of deregulated genes was identified. Functional clustering analysis performed on these genes generated four main factors: antigen processing and presentation, with its major histocompatibility complex-II—related genes; genes correlated with the cytotoxic activity of immune system; T-cell chemotaxis/cell adhesion genes; and T-CD4$^+$ regulator cell—related genes. A deregulation score (DS) was calculated for each sample. On the basis of their DS, tumors were then classified as COLD ($DS \leq -3$) to select the samples with a strong down-regulation of the immune system and NOT COLD ($DS \geq -2$). The COLD group of patients showed a worse prognosis in terms of survival considering all patients ($P = 0.0172$) and patients with metastatic disease ($P = 0.0031$). These results confirm that dMMR-CRCs do not constitute a homogeneous group as concerns the immune system activity of tumor microenvironment. In particular, the distinction between COLD and NOT COLD tumors may improve the management of these two subsets of patients. *(J Mol Diagn 2020, 22: 685—698; https://doi.org/10.1016/j.jmoldx.2020.02.008)*

The defective function of the mismatch repair (MMR) system causes the accumulation of gene mutations, such as insertions or deletions that induce an increase of neoantigens and elicit a remarkable endogenous antitumor immune response. Microsatellite instability (MSI) is a phenotypic marker of the deficient DNA MMR system and drives the pathogenesis of approximately 15% of colorectal cancers (CRCs). The system is composed by four proteins (DNA mismatch repair protein Mlh1, DNA mismatch repair protein Msh2, DNA mismatch repair protein Msh6, and mismatch repair endonuclease PMS2) and is involved in the repair of DNA sequence mismatches that occur during DNA replication.[1] The active immune microenvironment is counterbalanced by the strong expression of immunosuppressive ligands and signals, including programmed death-1 (PD-1) and programmed death ligand-1 (PD-L1). For these reasons, MSI tumors represent an ideal model to assess the activity and efficacy of

R.G. and G.Z. contributed equally to this work.
Disclosures: None declared.

https://doi.org/10.1016/j.jmoldx.2020.02.008

checkpoint inhibitors. Indeed, pembrolizumab and nivolumab have shown impressive response rates and long-lasting survival in chemorefractory MSI metastatic CRC patients.[2–5] However, the studies assessing checkpoint blockade immunotherapies in MSI metastatic CRC have demonstrated that only half of these patients benefited from anti–PD-1 inhibitors, despite the strong biological rationale.[3,5] One possible explanation for this different efficacy of checkpoint inhibitors could be because of the immune-microenvironment heterogeneity of MSI CRCs.

In other cancer types, such as melanoma, which present high mutational burden, gene expression profiling has allowed to detect two major phenotypes of tumor microenvironment: a T-cell–inflamed phenotype, characterized by the expression of T-lymphocyte markers and chemokines correlated with the recruitment of T lymphocytes; and a non–T-cell–inflamed phenotype missing the expression of immune-related genes. Typically, the T-cell–inflamed phenotype is also characterized by high representation of immune-inhibitory factors, including expression of the membrane protein PD-L1, expression of the tryptophan-catabolizing enzyme indoleamine 2,3-dioxygenase 1, and infiltration of forkhead box protein P3–positive T-regulatory (Treg) lymphocytes, which indicate the occurrence of immune escape in the context of an antitumor immune response.[6–12] Patients presenting a T-cell–inflamed immune phenotype respond better to different immunotherapeutic approaches, such as anticancer vaccines, high-dose IL-2, and inhibitory antibodies directed against cytotoxic T-lymphocyte associated-4, PD-1, and PD-L1.[13] Preclinical studies and *in vivo* analysis of specific biomarkers have suggested that the therapeutic activity of these immunotherapies is associated with the reactivation in the tumor microenvironment of T lymphocytes capable of recognizing tumor antigens.[14] On the basis of these considerations, an mRNA expression analysis was performed to describe the immune profile of deficient MMR (dMMR) CRCs.

Materials and Methods

Tissue Selection and Histologic Revision

Primary tumor samples [formalin fixed, paraffin embedded (FFPE)] of 89 dMMR CRC patients referred to two Italian Oncology Units (Azienda Ospedaliero–Universitaria Pisana, Pisa, Italy; and National Cancer Institute, Milan, Italy) were collected from 2012 to 2017.

CRCs were selected according to the absence of the protein expression encoded by the corresponding MMR genes (*hMLH1*, *hMSH2*, *hMSH6*, or *PMS2*), which reflects the MSI phenotype.

The most representative paraffin block of each sample was selected for analysis with necrosis areas and regression zones excluded. The study was conducted anonymously and in compliance with the principles of the Declaration of Helsinki of 1975.

Nucleic Acid Extraction and Purification

For each sample, four unstained sections (5 μm thick) were used for RNA extraction. The unstained sections were deparaffinized with xylene and rehydrated in decreasing-grade ethanol solution. Manual microdissection was performed to maximize the amount of tumor cells. RNA was isolated by using the RNeasy FFPE Kit (Qiagen, Hilden, Germany), according to the manufacturer's instructions. RNA was eluted in 20 μL of RNase-free water. RNA quantity and quality were assessed by means of a spectrophotometer (Xpose Trinean, Gentbrugge, Belgium).

Immune-Related Gene Expression Analysis

Analysis of the expression profiles of >700 immune-related genes was performed by the nanoString nCounter PanCancer Immune Profiling Panel (NanoString Technologies, Seattle, WA).

In detail, 150 ng of RNA from each sample was hybridized with the nCounter PanCancer Immune Profiling Panel (GX Assay) CodeSet. All the procedures related to mRNA quantification, including sample preparation, hybridization, detection, and scanning, were performed following the manufacturer's instructions. The counts were normalized according to the standard protocol. Raw nanoString counts for each mRNA within each experiment were subjected to technical normalization with the counts obtained for positive-control probe sets before biological normalization using the 40 reference genes included in the CodeSet. The normalized data were log2 transformed and then used as input for differential expression analysis. The data were filtered to exclude relatively invariant features and features below the detection threshold (defined for each sample by a cutoff value corresponding to twice the SD of the negative control probes plus the means).

mRNA Expression Data Analysis

The PanCancer Immune Profiling Advanced Analysis Module (NanoString Technologies) was used to conduct the statistical analyses of data obtained by the nCounter panel analysis. The analysis module grouped the genes into functional immune-related categories (namely, transporter functions, tumor necrosis factor superfamily, macrophage functions, antigen processing, adhesion, regulation, T-cell functions, cytokines, B-cell functions, ILs, toll-like receptor, cytotoxicity, pathogen defense, cancer/testis antigens, complement, natural killer (NK) cell functions, cell functions, chemokines, leukocyte functions, cell cycle, senescence, and microglial functions).

To understand what the immune cell profiling results represented, a set of genes for each cell population was assumed to be specific (reference genes) to that cell type. This assumption allowed measuring the abundance of a cell type by simply taking the average log2 expression of its

characteristic genes. This approach was used to test the relative abundance of B cells, T cells (helper T cells, Tregs, cytotoxic cells, $CD8^+$ T cells, and CD45), natural killer cells, dendritic cells, macrophages, mast cells, and neutrophils.[15,16]

To investigate the differential expression between the samples in this study, the main covariates considered were tumor size, tumor stage, and presence of metastases and molecular profile of the samples. The large number of genes in the CodeSet made the use of raw *P* values problematic. Therefore, the Benjamini-Yekutieli false discovery rate correction was used for adjusting *P* values; genes with a fold change ≥ 1 and a Benjamini-Yekutieli false discovery rate < 0.05 were considered differentially expressed.

Functional Clustering Analysis and Factor Classification

Functional clustering analysis was performed starting from the immune-related categories of genes revealed by Pan-Cancer Immune Profiling Advanced Analysis to confirm, and relates to the immune cell population in the observed clusters. Analysis was performed by DAVID Bioinformatics Resources 6.8 and STRING version 10.5.[17] to evaluate the gene expression and the corresponding potential protein networks. The Markov Cluster algorithm with inflation = 3 was used to group the genes into annotation clusters on the basis of precomputed similarity information.[18] In addition, vector quantization (k-means clustering) with applied number of clusters was revealed. The resulting clusters were annotated and ranked by linear *P* value (Pearson) with Bonferroni's correction using a threshold of counted genes.

Preliminary basic clusters ($P < 0.05$) were selected for further analysis to determine a strong gene signature correlated with the different immune cell population and their mechanism of action. R-linear correlation analysis of the gene expression levels of the singular clusters with Bonferroni's correction was performed in Past software version 3.21 (*https://folk.uio.no/ohammer/past*, last accessed October 1, 2018), generating four subsets with strongly correlated genes belonging to the same functional clusters. A refinement and reclassification of the new functional cluster's groups generated was performed by the association of the immune cell types and the corresponding functions generating the final determinant factors.

Sample Classification on the Basis of Quartile Clustering Technique

A sample classification was performed using the quartile clustering technique on the basis of the factors determined by functional clustering analysis and gene expression values (from nCounter).[19,20] Quartiles are a major tool in descriptive analysis, which divides the range of data into three parts. Once the values of upper quartile, median quartile, and lower quartile had been determined for a singular clustered gene, the discrete value was assigned according to the affiliation of the experimental value of gene expression to the specific interquartile range.

Calculation of the total score for each of the functional clusters was based on the algebraic sum of the partial grades ($\sum g$) and was assigned in a discrete way using the following condition: -1 if $\sum g < 0$; 0 if $\sum g = 0$; and $+1$ if $\sum g > 0$.

Statistical Analysis

Data were analyzed using both parametric and nonparametric tests using Statistica software version 12 (StatSoft, Tulsa, OK) and Past software.

The log-rank test (Statistica Software) was used to compare the Kaplan-Meier survival curves of each immune profile group of patients. Three distinct overall survivals were calculated from the following: i) date of the first cancer diagnosis of CRC for all patients (OS); ii) date of the first cancer diagnosis of CRC for nonmetastatic patients; and iii) date of the diagnosis of metastatic disease for metastatic patients (OS-MetDis) until death attributable to any cause. Because of the issue of multiplicity (three hypotheses), the Bonferroni correction was used and the significance threshold was set to be 0.0167.

Immunohistochemical Analysis, Staining Scores, and $CD3^+/CD8^+$ LyD

In a subset of 39 patients, immunohistochemical analysis of CD3 and CD8 expression was performed on FFPE tumor sections by using rabbit monoclonal CONFIRM anti-CD3 ready-to-use antibody clone 2GV6 or rabbit monoclonal CONFIRM anti-CD8 antibody clone SP57; sections were stained using the BenchMark ULTRA IHC/ISH System (all from Roche-Ventana Medical Systems, Tucson, AZ).

The different marker expression in lymphocytes and in tumoral cells was evaluated independently by two investigators (C.U. and G.F.) on 10 high-power fields ($\times$40 magnification) of tumoral core (CT) and on 10 high-power fields of infiltrative tumoral margins (IMs). The mean value of the different fields was then calculated.

The overall $CD3^+$ and $CD8^+$ lymphocyte density (LyD) within the CT and the IM tumor compartments was calculated as follows: the mean of the four percentiles obtained for each marker (CD3 and CD8 mean counts at either CT or IM) was translated into three groups (low, intermediate, and high) corresponding to mean percentiles of 0% to $<$25%, $\geq$25% to $<$70%, and $\geq$70% to 100%, respectively.[21]

Immunohistochemical analysis of PD-1 and PD-L1 expression was performed on FFPE tumor sections using PD-1 (clone NAT105) mouse monoclonal antibody (Roche-Ventana Medical Systems) and PD-L1 (clone S263) Assay (rabbit monoclonal primary antibody) ready-to-use (Roche-Ventana Medical Systems). Sections were stained using the BenchMark ULTRA IHC/ISH System.

The PD-1 and PD-L1 expression was evaluated in both lymphocytes and tumoral cells independently by two

Table 1 Functional Clustering Results, Descriptive Statistics, and Quartile Determination of the Analyzed Gene Sets

		Clustering of the sets			Descriptive statistic			Quartile of gene expression		
Factor	mRNA	Gene description	FDR *P* value	Acronym	Mean*	Median*	Range*	Quartile 2*	Quartile 1*	Quartile 3*
1. Antigen processing and presentation	*CD74*	CD74 molecule	1.18×10^{-5}	MHC-II	13.33	13.43	10.50–15.07	13.43	12.47	14.05
	HLA-DMA	DM α	1.18×10^{-5}		9.92	9.83	7.25–12.25	9.86	9.02	10.78
	HLA-DPA1	DP α 1	1.18×10^{-5}		11.12	11.23	8.47–13.08	11.15	10.04	12.13
	HLA-DPB1	DP β 1	1.18×10^{-5}		10.52	10.54	8.25–12.39	10.51	9.66	11.58
	HLA-DRB3	DR β 3	1.18×10^{-5}		12.91	12.87	10.76–14.84	12.77	12.24	13.70
2. NK/T-cell–mediated cytotoxicity	*CD8A*	CD8a molecule	3.09×10^{-2}	Tc	7.20	7.27	1.12–10.21	7.29	6.24	8.29
	PRF1	Perforin 1	3.09×10^{-2}		8.06	8.17	1.52–10.22	8.11	7.22	9.11
	GZMA	Granzyme A	3.09×10^{-2}		8.43	8.46	1.52–11.12	8.41	7.27	9.62
	GZMB	Granzyme B	3.09×10^{-2}		8.13	8.16	1.52–10.76	8.16	7.04	9.35
	GZMK	Granzyme K	3.09×10^{-2}		6.89	6.97	1.52–9.55	7.02	5.91	7.96
	CD3D	CD3d molecule	3.09×10^{-2}		7.90	7.98	5.14–9.87	7.93	7.01	8.67
	CD3E	CD3e molecule	3.09×10^{-2}		7.23	7.43	1.12–9.36	7.41	6.245	8.07
	CD27	CD27 molecule	3.09×10^{-2}		7.12	7.27	1.52–9.55	7.20	6.065	8.08
	CD2	CD2 molecule	3.09×10^{-2}		5.49	5.59	1.12–7.83	5.53	4.94	6.53
	CD28	CD28 molecule	3.09×10^{-2}		4.86	5.00	1.12–7.09	4.94	4.335	5.64
	CD40L	CD40 ligand	3.09×10^{-2}		5.09	5.08	1.52–7.51	7.07	5.145	8.73
	ITGAL	Integrin subunit α L	3.09×10^{-2}		7.81	7.90	5.24–9.65	7.83	6.855	8.57
	CD80	CD80 molecule	3.09×10^{-2}		5.66	5.77	1.52–8.07	5.71	5.19	6.41
3. T-cell chemotaxis	*CXCL9*	C-X-C motif chemokine ligand 9	1.62×10^{-5}	CAdh	10.02	10.19	6.28–12.96	10.19	8.945	11.31
	CXCL10	C-X-C motif chemokine ligand 10	1.62×10^{-5}		8.12	7.98	1.12–11.97	7.98	7.055	9.66
	CXCL11	C-X-C motif chemokine ligand 11	1.62×10^{-5}		8.50	8.38	1.52–12.17	8.38	7.1	10.14
	KLRC1	Killer cell lectin-like receptor C1	1.62×10^{-5}		5.54	5.57	1.52–7.67	5.57	4.855	6.21
	KLRC2	Killer cell lectin-like receptor C2	1.62×10^{-5}		6.37	6.49	1.12–8.84	6.49	5.66	7.27
	KLRD1	Killer cell lectin-like receptor D1	1.62×10^{-5}		5.46	5.60	1.52–7.69	5.60	4.905	5.98
4. Regulation of $CD4^+$ T cells	*CD4*	CD4 molecule	1×10^{-4}	Treg	7.71	7.81	1.52–9.91	7.82	7.27	8.32
	CTLA-4	Cytotoxic T-lymphocyte associated protein 4	1×10^{-4}		7.20	7.29	1.52–9.10	7.18	6.45	8.33
	IL2RA	IL-2 receptor subunit α	1×10^{-4}		5.27	5.05	1.12–8.13	7.71	6.84	8.51
	LAG3	Lymphocyte activating 3	1×10^{-4}		6.90	6.95	1.12–9.48	6.86	6.025	8.13

*Log2 normalized counts.

CAdh, cell adhesion; FDR, Benjamini-Yekutieli false discovery rate; MHC, major histocompatibility complex; NK, natural killer; Tc, cytotoxic T lymphocyte; Treg, T-regulatory.

investigators (C.U. and G.F.) by considering one stained section entirely for each sample. PD-1 and PD-L1 expression in both tumor cells and lymphocytes was annotated as the estimated percentage of stained cells and was categorized as follows: negative/low (<1% stained tumor cells) and high (1% to 100% stained tumor cells).[22]

Results

Sample Features

The clinical and pathologic characteristics of the samples included in the present study are the following: clinicopathologic stage at the time of diagnosis, primary tumor sidedness, presence of metastases, and, when available, presence of *RAS* or *BRAF* mutations.

Seven dMMR CRCs were stage I, 45 were stage II, 15 were stage III, and 22 were stage IV at the time of diagnosis.

Sixty-seven dMMR CRCs were right sided, and 22 were left sided; right-sided tumors were defined as arising from the cecum to the transverse colon, and left-sided tumors were defined as arising from the splenic flexure to the rectum.

dMMR CRCs were divided into synchronous, metachronous, and nonmetastatic disease, with synchronous metastatic disease defined as distant metastasis occurring within 3 months since the primary diagnosis, metachronous metastatic disease defined as distant metastasis occurring beyond 3 months since the primary diagnosis, and nonmetastatic disease defined for the patients without metastases with at least 3

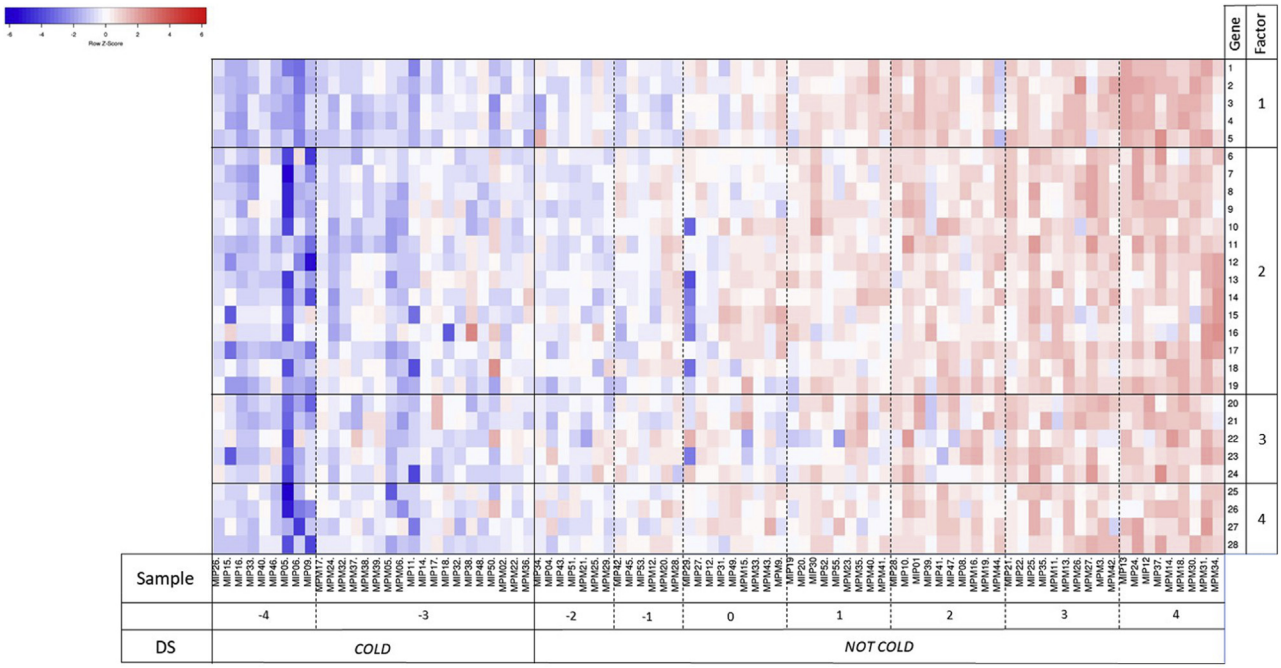

Figure 1 Expression heat maps of the genes related to the four factors, together with deregulation score (DS) information. Genes: (1) *CD74*; (2) *HLA-DMA*; (3) *HLA-DPA1*; (4) *HLA-DPB1*; (5) *HLA-DRB3*; (6) *CD8A*; (7) *PRF1*; (8) *GZMA*; (9) *GZMB*; (10) *GZMK*; (11) *CD3D*; (12) *CD3E*; (13) *CD27*; (14) *CD2*; (15) *CD28*; (16) *CD40L*; (17) *ITGAL*; (18) *CD80*; (19) *CXCL9*; (20) *CXCL10*; (21) *CXCL11*; (22) *KLRC1*; (23) *KLRC2*; (24) *KLRD1*; (25) *CD4*; (26) *CTLA-4*; (27) *IL2RA*; and (28) *LAG3*. Factors: (1) antigen processing and presentation; (2) natural killer/T-cell–mediated cytotoxicity; (3) T-cell chemotaxis; and (4) regulation of $CD4^+$ T cells.

years of follow-up.[23] In detail, 22 MMR CRCs were synchronous metastatic disease, 14 were metachronous metastatic disease, and 53 were nonmetastatic disease.

Mutational status was known for 81 samples: 38 samples (46.9%) harbored a mutation within the *BRAF* gene (exon 15), 25 samples (30.9%) harbored a mutation within *K-RAS* or *N-RAS* genes (exons 12, 13, 61, 117, and 146), whereas 18 samples (22.2%) resulted to be wild type for both genes.

Data Normalization, Gene Expression, and Functional Immune-Related Categories

The housekeeping genes selected for the normalization of the experiment presented a steady expression level in all the studied samples (data not shown). None of the samples was excluded after data normalization.

Supplemental Figure S1 shows the heat maps of the mRNA normalized data, scaled to give all genes equal variance, generated via unsupervised clustering. Orange indicates high expression; blue indicates low expression. This plot is meant to provide a high-level exploratory view of the data. In detail, Supplemental Figure S1 shows the heat map displaying each sample level of the mRNA expression of all genes included in the Immune Profile Panel without any evidence of an overall mRNA expression clustering. Supplemental Figure S2 shows the heat maps displaying each sample level of expression of antigen processing, cytotoxicity, natural killer cell function, and T-cell functional groups of genes. All the 206 genes included in the four immune categories were then analyzed and classified by gene-expression functional clustering.

Factor Determination by Gene-Expression Functional Clustering

Determination of the factors inside the immune profile panel analyzed plays a critical role in the elucidation of the linkage and mechanism between the immune system and the tumor samples analyzed. Therefore, a gene expression functional analysis was performed, generating four main factors denominated by ordinal number: 1, 2, 3, and 4 (Table 1). Factor 1 contains five genes constituting the antigen processing and presentation class II. Factor 2, composed by 13 entities, contains genes preferentially expressed in cytotoxic cells as surface markers in T cells, NK cells, and δγ T cells and gene-expressing inducer of cytolysis. Factor 3 is characterized by six genes involved in T-cell chemotaxis/cell adhesion. Finally, factor 4 contains four genes expressed in T-$CD4^+$ regulator cells (Tregs). In summary, the results obtained from functional clustering analysis showed the antigen processing and presentation mechanism, $CD4^+$ (Treg) population, cytotoxic activity, and cell adhesion as main functions of the immunity system in the samples analyzed.

Quantitative Analysis of the Functional Factors by Quartile Clustering Technique

To define the magnitude of activity of the four functional factors previously determined in relation to the analyzed

Table 2 Molecular Classification and Clinical Pathologic Characteristic Association

Variable	COLD		NOT COLD		P value*
	N	%	N	%	
Localization					
Left	12	42.9	10	16.4	**0.0088**
Right	16	57.1	51	83.9	
Genotype†					
WT	7	28.0	11	19.6	
RAS‡	6	24.0	19	33.9	0.2375
BRAF‡	12	48.0	26	46.4	0.4021
Tumor stage					
I	1	3.6	6	9.8	**0.0373**
II	11	39.3	34	55.7	(I and II vs
III	9	32.1	6	9.8	III and IV)
IV	7	25.0	15	24.6	
Metastatic status					
Yes	14	50.0	22	36.1	0.1560
No	14	50.0	39	63.9	

Bold indicates statistical significance.
*Fisher exact P value, one tailed (Statistica Software).
†Available for 81 samples.
‡K-RAS or N-RAS genes (exons 12, 13, 61, 117, and 146), BRAF gene (exon 15).
WT, wild type.

samples, a quartile clustering technique has been used. For each of the factors and samples, a discrete value between −1 (low activity), 0 (medium activity), and 1 (high activity) has been assigned (*Materials and Methods*) based on the relative gene expression levels. Factor 1 [antigen processing and presentation, major histocompatibility complex (MHC)-II] showed down-regulation in 32 (36%) samples and up-regulation in 24 (27%). Factor 2, containing genes correlated with cytotoxic activity of the immune system, showed a slight difference between samples showing high activity (36; 40%) and low activity (32; 38%). Factor 3 (T-cell chemotaxis/cell adhesion) showed a large predominance of down-regulated genes (47; 51%) with respect to up-regulated samples (25; 28%). Finally, factor 4 ($CD4^+$ Treg) displayed a uniform distribution between up-regulated (30; 32%) and down-regulated (28; 34%) samples.

Tumor Classification

Tumor classification was performed using the results achieved from the quantitative quartile clustering of the samples described above. The algebraic sum of the discrete values of the singular factors was calculated, and a deregulation score (DS) with a value between −4 and 4 was determined for each sample. First, two groups of tumors samples were generated, on the basis of the DS values: COLD and NOT COLD.

The COLD group contains tumor samples with a DS value ≤ -3 to select the samples with a strong down-regulation of the immune system; the NOT COLD group includes samples having a DS ≥ -2 with an incomplete down-regulation or with at least a partial up-regulation of the immune system. The NOT COLD samples were subdivided into an INTERMEDIATE group, with a DS ranging from −2 to 2, and a HOT one, with a DS >2.

On the basis of the tumor classification described above, 28 tumor samples were classified as COLD and 61 were classified as NOT COLD, representing 31.5% and 68.5% of the total samples, respectively (Figure 1 and Supplemental Table S1). Tables 2 and 3 summarize the distribution of COLD and NOT COLD, and COLD, INTERMEDIATE, and HOT samples, respectively, with respect to localization, genotype, tumor stage, and metastatic status.

Differential Gene Expression Analysis

Compared with COLD samples, NOT COLD samples showed a statistically significant expression deregulation in a series of genes listed in Supplemental Table S2. These findings were visualized in the specific Volcano plot (Supplemental Figure S3A) of all of the data displaying each log10 gene (*P* value) and log2 fold change for COLD samples compared with NOT COLD ones. In addition, the classification considering the COLD, INTERMEDIATE, and HOT immune profile status is in line with the extent of gene expression deregulation within these three groups. The lists of deregulated genes between INTERMEDIATE versus COLD and HOT versus COLD are reported in Supplemental Tables S3 and S4 and visualized in two related Volcano plots (Supplemental Figure S3, B and C).

Conversely, the analyses for the comparison of the expression between right-sided versus left-sided dMMR CRCs; stages II, III, and IV versus stage I dMMR CRCs; mutated (*KRAS*, *NRAS*, or *BRAF*) versus nonmutated dMMR CRCs; and metachronous metastatic disease, synchronous metastatic disease versus nonmetastatic disease dMMR CRCs failed to display statistically significant gene-expression changes, showing only marginal equability between up-regulated and down-regulated genes.

Association between Immune Profile and OS

The log-rank (Mantel-Cox) test allowed us to observe a statistically significant difference in OS-MetDis Kaplan-Meier survival curves between the COLD and NOT COLD patients (Figure 2E) with a *P* value of 0.0031; the hazard ratio was 6.921 (95% CI, 1.92−24.91). On the other hand, no significant differences ($P = 0.0172$ and $P = 0.3494$) were observed for either all patients or the nonmetastatic patients (Figure 2, A and C), with hazard ratios of 4.174 (95% CI, 1.28−13.52) and 0.239 (95% CI, 0.01−4.90), respectively. Considering the COLD, INTERMEDIATE, and HOT immune-profile classification, the survival comparison between the three groups (Figure 2, B, D, and F) was not significant. Potential confounders, such as age, sex,

Table 3 Molecular Classification and Clinical Pathologic Characteristic Association

	COLD		INTERMEDIATE		HOT		
Variable	*N*	%	*N*	%	*N*	%	*P* value*
Localization							
Left	12	42.9	9	21.4	1	5.3	**0.0028**
Right	16	57.1	33	78.6	18	94.7	
Genotype†							
WT‡	7	28.0	8	20.5	3	17.6	
RAS‡	6	24.0	13	33.3	6	35.3	0.3158
BRAF‡	12	48.0	18	46.2	8	47.1	0.5753
Tumor stage							
I	1	3.6	3	7.1	3	15.8	**0.0066**
II	11	39.3	21	50.0	13	68.4	(I and II vs III and IV)
III	9	32.1	6	14.3	0	0.0	
IV	7	25.0	12	28.6	3	15.8	
Metastatic status							
Yes	14	50.0	17	40.5	5	26.3	0.1134
No	14	50.0	25	59.5	14	73.7	

Bold indicates statistical significance.
**U*-test, adjusted (Statistica Software).
†Available for 81 samples.
‡*K-RAS* or *N-RAS* genes (exons 12, 13, 61, 117, and 146), *BRAF* gene (exon 15).
WT, wild type.

and mutational status, did not affect the final results obtained by Kaplan-Meyer survival analysis, whereas the survival outcome result was affected by the presence of a metastatic disease (or a higher stage disease) and the hazard ratio of Cox regression analyses is reported in a supplemental figure (Supplemental Figure S4).

Lymphocyte Density

$CD3^+$, $CD8^+$ LyD within the CT and IM tumor compartments was as follows: 8 samples (21%) revealed a high LyD, 23 samples (59%) revealed an intermediate LyD, and 8 samples (21%) revealed a low LyD. A higher LyD was significantly associated with the NOT COLD immune phenotype ($P = 0.0412$) (Figure 3A). Considering the three immune phenotype classes, LyD was significantly higher in HOT than in COLD samples ($P = 0.0081$) and in HOT compared with INTERMEDIATE samples ($P = 0.0216$), whereas no significant LyD differences were observed between COLD and INTERMEDIATE samples (Figure 3B).

PD-1 Expression

PD-1 expression in neoplastic cells was reported in 4 of 39 analyzed samples (10.0%); two of the PD-1 positive samples were COLD, and the other two were NOT COLD (one INTERMEDIATE and one HOT). Considering the LyD, the four PD-1 positive samples were two LyD high, one LyD intermediate, and one LyD Low. The PD-1 expression in lymphocytes was reported in 36 of 39 analyzed samples (92.3%).

PD-L1 Expression

PD-L1 expression in neoplastic cells was reported in 19 of 39 analyzed samples (48.7%), and no differences were observed between the COLD and the NOT COLD samples ($P = 0.9192$, *U*-test with continuity correction), with seven positive and seven negative and 12 positive and 13 negative samples, respectively (Figure 4A).

Considering the molecular classification in three classes, there is no significant difference ($P = 0.7584$, *U*-test with continuity correction) in the rate of PD-L1 positive samples in neoplastic cells among COLD (50.0%; 7 of 14), INTERMEDIATE (42.1%; 8 of 19), and HOT samples (66.6%; 4 of 6) (Figure 4B). Similarly no significant difference was reported between the rate of PD-L1 positive neoplastic cells ($P = 0.3313$, *U*-test with continuity correction) among LyD low (50.0%; 4 of 8), LyD intermediate (39.1%; 9 of 23), and the LyD high samples (75.0%; 6 of 8) (Figure 4C).

The PD-L1 expression in the lymphocytes was positive in 31 of 38 analyzed samples (82%), and the expression distribution differed neither between COLD and NOT COLD samples nor between the three molecular and the LyD classes.

Discussion

Colorectal tumors with dMMR present well-defined common features from a clinical, histologic, and molecular point of view, with important prognostic and predictive implications. The high mutational load and the consequent high lymphocytic infiltration characterizing these tumors

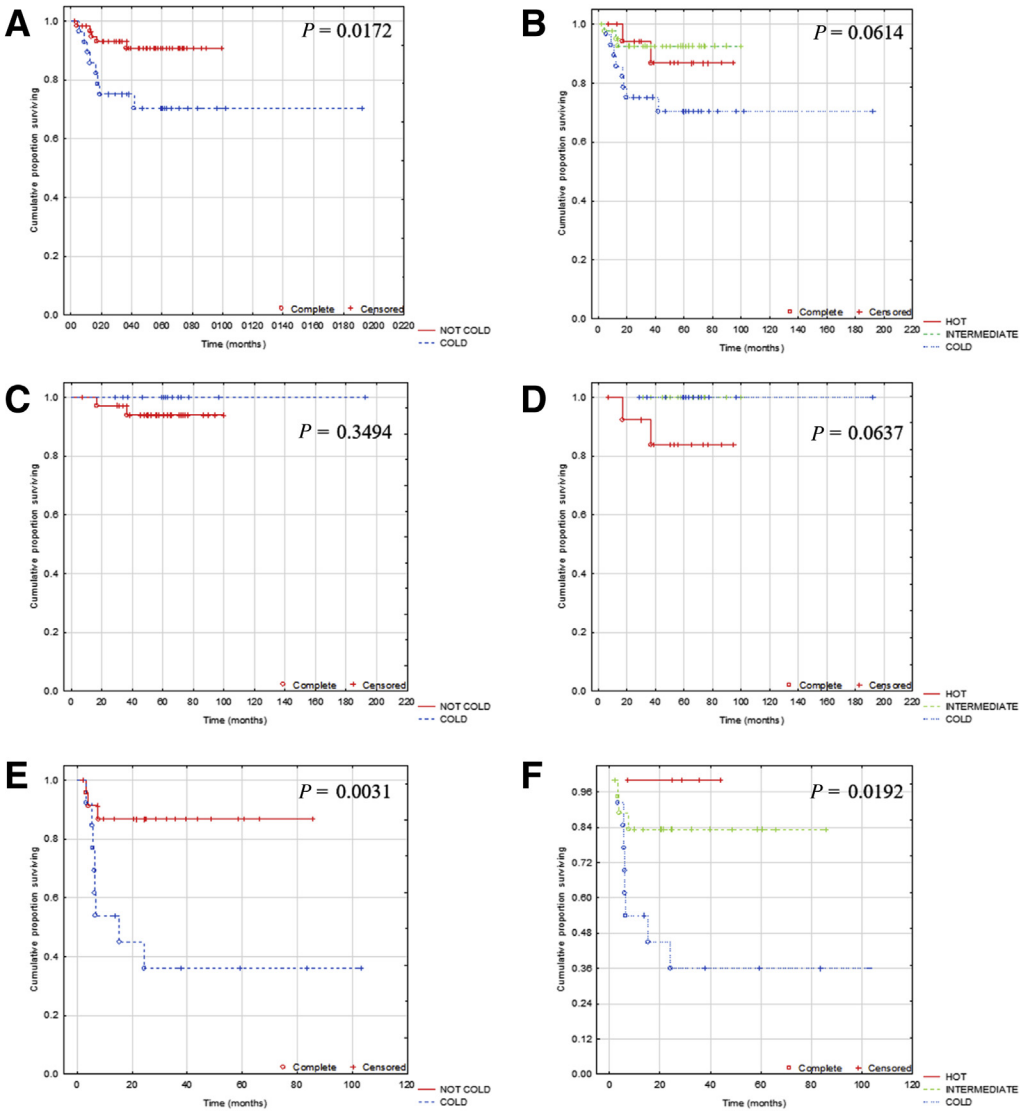

Figure 2 Kaplan-Meier survival curves between the COLD and NOT COLD immune profile classification: overall samples (**A**), nonmetastatic samples (**C**), and metastatic samples (**E**). Kaplan-Meier survival curves between the COLD, INTERMEDIATE, and HOT immune profile classification: overall samples (**B**), nonmetastatic samples (**D**), and metastatic samples (**F**).

constitute an important biological rationale regarding the efficacy of immunotherapy despite the fact that not all CRC dMMR patients benefit from treatment with checkpoint inhibitors. The dMMR CRC immunoprofile was evaluated on the basis of the gene expression data derived from other malignancies, like melanomas (that distinguish between inflamed and noninflamed tumors as probable predictive factors of immunotherapy efficacy), to obtain a comprehensive overview of the immune microenvironment of these tumors.[9–12] The high marked intratumoral infiltration and the inflammatory response in dMMR CRCs might be related to the genetic instability of this group of tumors.[24–26] As a matter of fact, the unreliable DNA repair in these tumors results in the production of many abnormal peptides (ie, tumor-specific antigens) that may trigger the immune system, including recruitment and activation of cytotoxic T cells. dMMR status is known to have a strong prognostic value. Stage I, II, and III CRC patients with dMMR CRC tumors are often found to have a more favorable prognosis,[1,27,28] and this may be partly explained by the benefit from T-cell infiltration.[24–26]

In this study, the NanoString nCounter analysis system was used for the immune gene expression profiling of a series of dMMR CRCs. High sensitivity combined with absence of the amplification step using the nCounter technology was useful to determine the gene expression of the clinical FFPE tumor tissue samples.[29,30]

The analysis showed that the dMMR CRCs constitute a heterogeneous group from the point of view of immune microenvironment, with regard to the gene expression of

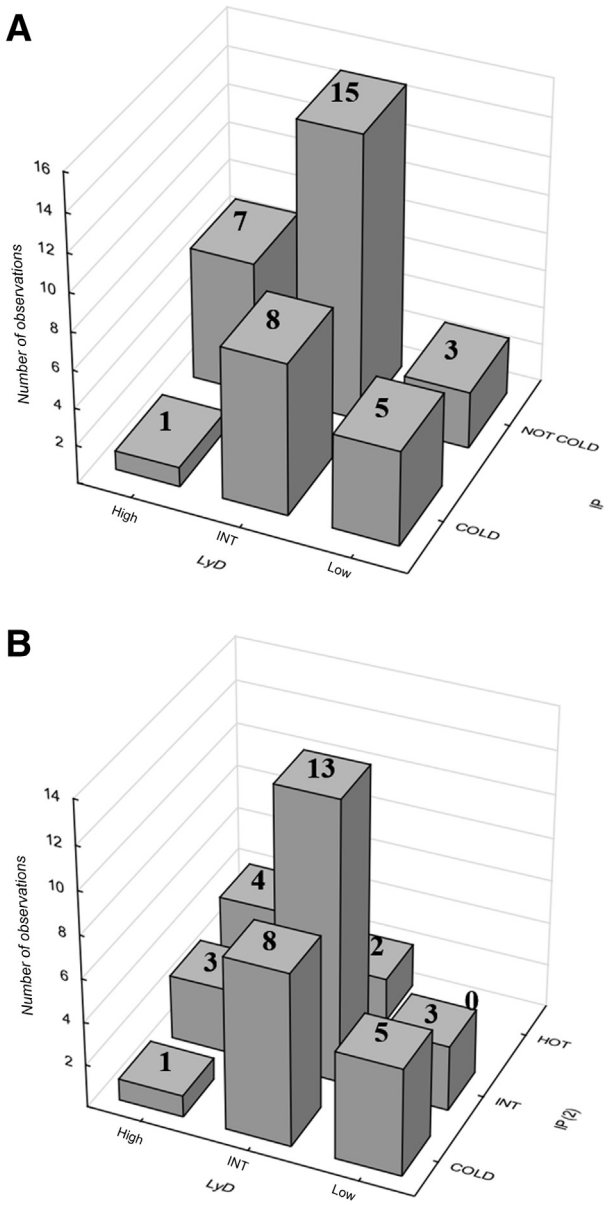

Figure 3 **A:** Correlations between COLD and NOT COLD immune profile classification and lymphocyte density (LyD; $P = 0.0412$). **B:** Correlations between COLD, INTERMEDIATE (INT), and HOT immune profile classification and LyD ($P = 0.0216$ HOT versus INT; $P = 0.0081$ HOT versus COLD). *U*-test with continuity correction was used. IP, immune profile.

some functional groups: antigen-presenting MHC-II, NK/T-cell–mediated cytotoxicity, T-cell chemotaxis, and $CD4^+$ T-cell regulation.

A gene mRNA expression data analysis of the relative abundances of the immune cell populations (B cells, T cells, natural killer cells, dendritic cells, macrophages, mast cells, and neutrophils), obtained from a panel of 770 immune-related genes, was performed to determine the clinical potential of gene-expression analysis, and to classify patients and their association with OS. Subsequently, a subset of 206 mRNAs were submitted to *in silico* meta and functional cluster analysis to determine the main factors underlying the immune behaviors/responses in the set of samples. As a result, a 28-gene expression signature related to the above-mentioned functions was obtained. The genes chosen to comprise this signature were differentially expressed by $CD3^+/CD8^+$ T cells and were highly variable across dMMR CRC tumor samples considered in this study. As an outcome of the *in silico* analysis, four main factors, factor 1 (antigen-presenting MHC-II), factor 2 (NK/T-cell–mediated cytotoxicity), factor 3 (T-cell chemotaxis), and factor 4 (regulation of $CD4^+$ T cells) (Table 1), were identified.

Factor 1 is characterized by the antigen processing and presentation (MHC-II) genes predominantly expressed in specialized antigen-presenting cells, such as dendritic cells and B cells, where they play a fundamental role in triggering the immune responses.[31–33] The analysis of the expression averages of genes belonging to factor 1 showed a progressive decrease in value from stage I to stage IV, and from right versus left (right expression higher than left). A strong correlation was observed in the samples between the genes belonging to factor 1 and the molecular characteristic of B cells, highlighting the role of the latter as major antigen-presenting cell population.

Factor 2 has positive loadings for genes that are involved in NK/T-cell–mediated cytotoxicity,[34,35] and is composed by the higher number of genes along the four observed factors (13 genes) representing 50% of the total 26-gene expression signature selected in this study. Compared with factor 1, which has cellular activators (MHC-II) of immune response, the genes in this group have downstream roles representing an active step in controlling tumor cell growth by their cytotoxic activity. As for factor 1, the mean of the gene-expression level in this group is higher in stages I and II than in stages III and IV.[36]

Factor 3 is characterized by positive loadings for chemokines (CXCL 9, 10, and 11) and killer cell receptors (NKG2-A/NKG2-B type II integral membrane protein, NKG2-C type II integral membrane protein, and natural killer cells antigen CD94), which represent key factors in the regulation of T-cell/NK cell chemotaxis.[37–39]

Finally, factor 4 is characterized by four genes involved in $CD4^+$ T-cell regulation. In this study, the gene-expression levels of these four genes constituting factor 4 showed a strong correlation along with the clinical stages of the tumors, as in the case of the previous factors.[33,40]

In summary, the *in silico* meta and clustering analysis approach together with the determination of the factors described above delineated a smaller set of supervariables by using gene-gene intercorrelations from a larger number of individual genes. In dMMR CRCs, a higher occurrence of the gene expression correlated with T cells ($CD4^+$ and $CD8^+$)/NK cells. This occurrence was greater in the lower stages (I and II) of cancer than in stages III and IV, which agrees with previous studies concerning the MSI colon cancer type.[1]

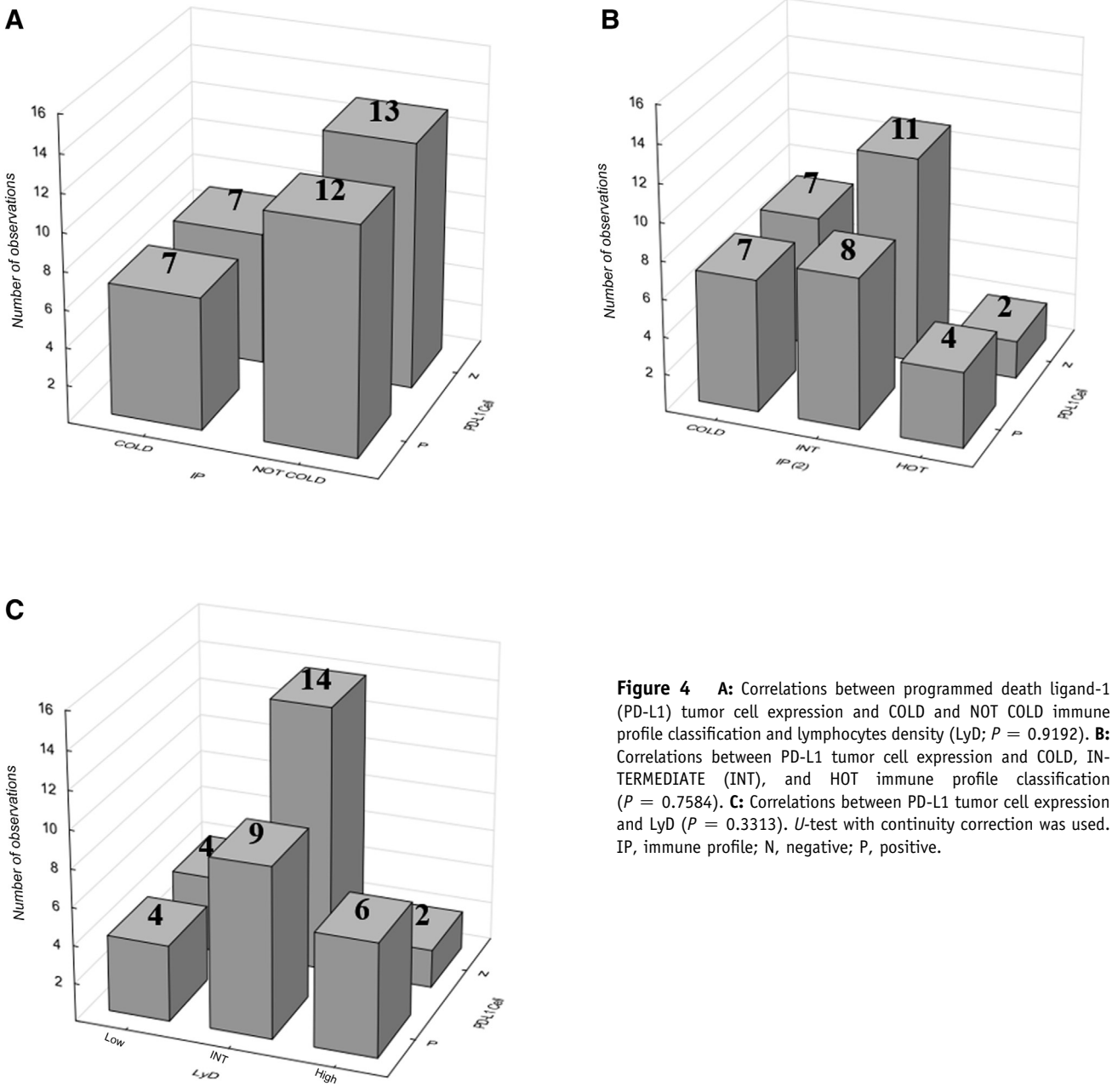

Figure 4 **A:** Correlations between programmed death ligand-1 (PD-L1) tumor cell expression and COLD and NOT COLD immune profile classification and lymphocytes density (LyD; $P = 0.9192$). **B:** Correlations between PD-L1 tumor cell expression and COLD, INTERMEDIATE (INT), and HOT immune profile classification ($P = 0.7584$). **C:** Correlations between PD-L1 tumor cell expression and LyD ($P = 0.3313$). *U*-test with continuity correction was used. IP, immune profile; N, negative; P, positive.

The overall quantitative evaluation of the expression of these 28 genes allowed building a classifier able to distinguish in a dichotomous way the so-called COLD tumors (which show a significant down-regulation of genes related to the immune system) from the so-called NOT COLD tumors, which show a complete or partial up-regulation of these genes (Table 2 and Figure 5). A further classification has distinguished the NOT COLD group in an INTERMEDIATE subgroup, with a partial activation of the immune response, and in a HOT subgroup, with great activation of the immune response. These groups differ from some points of view: as concerns the clinicohistopathologic characteristics, even if not in a statistically significant way, COLD tumors appear to occur more frequently in the more advanced stages of the disease and in the left colon. COLD tumors also show a clear down-regulation of several immunorelated genes and have a different prognosis, with lower overall survival, considering both the totality of patients (OS) and the patients with metastatic disease (OS-MetDis), whereas no significant differences were found when comparing the two groups of patients with nonmetastatic disease. Considering the classification in COLD, INTERMEDIATE, and HOT immune profile, the survival comparison among the three groups was significant only for metastatic disease.

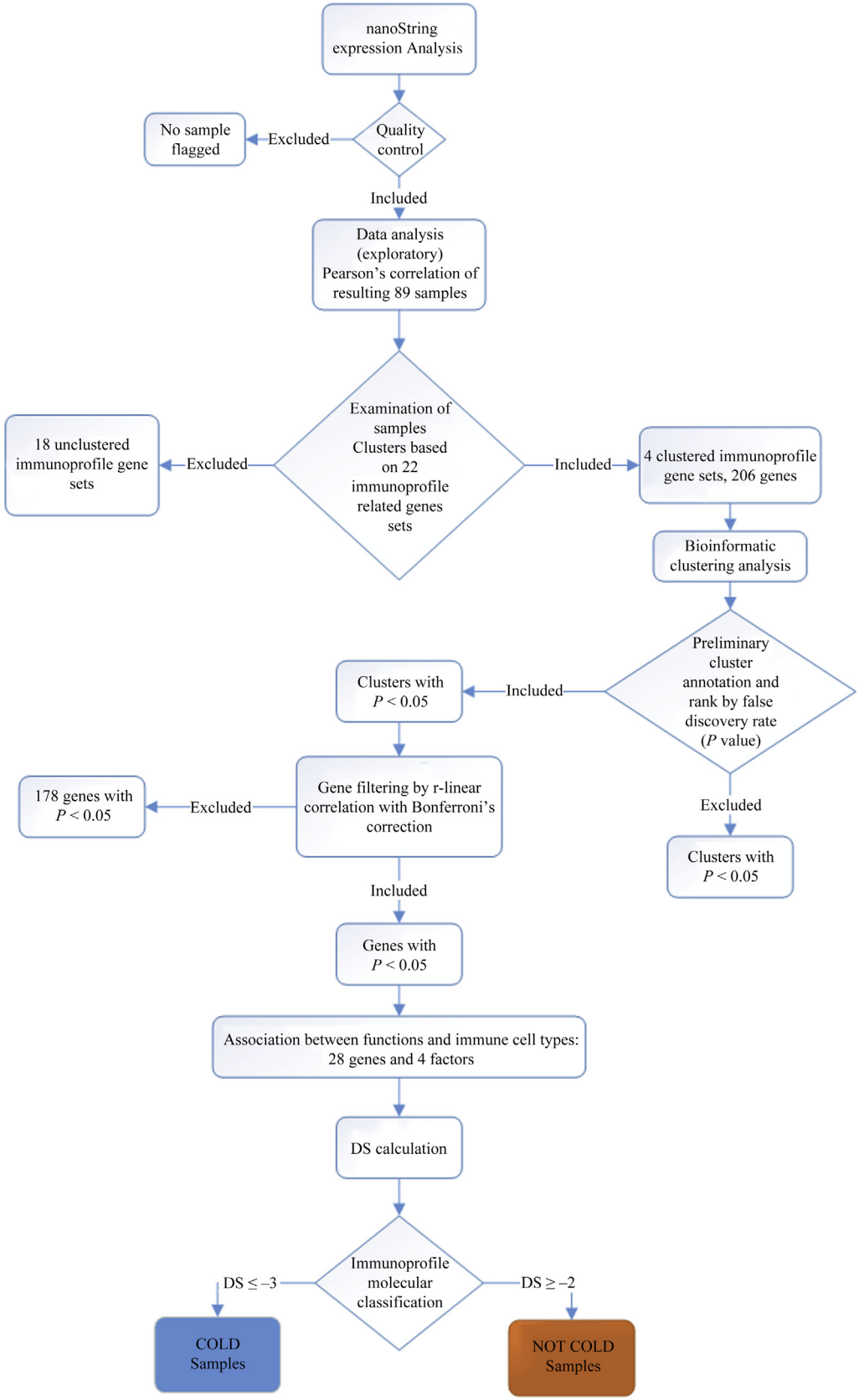

Figure 5 Flowchart of the experimental design for immunoprofile molecular classification of 89 deficient mismatch repair colorectal cancers. DS, deregulation score.

The molecular immune signatures were then compared with the tumor-infiltrating lymphocytes in a subset of samples. Tumor-infiltrating lymphocytes constitute the predominant immune cell populations in the tumor microenvironment. Tumor-infiltrating lymphocytes belong to both the adaptive and innate arms of the immune system. Different immune profiles have been proposed as prognostic and predictive factors; indeed, the immune infiltration at the tumor site may indicate a host response. Significant correlations were demonstrated between the levels of immune cell infiltration in tumors and patients' clinical outcome. Strong lymphocytic infiltration associated with good clinical outcome has been reported in many different tumors, including colorectal cancers.[41]

Recently, CRCs characterized by high density of T cells ($CD3^+$), of cytotoxic T cells ($CD8^+$), and of memory T cells ($CD45RO^+$) have been associated with longer disease-free (after surgical resection of the primary tumor) and/or overall survival.[42] Consequently, an immune classification of tumors was proposed on the basis of an immune score, performed by the quantification of two lymphocyte populations (CD3/CD8, CD3/CD45RO, or CD8/CD45RO), both in the core of the tumor (CT) and in the invasive margin (IM) of the tumor, to establish a prognosis of clinical outcome in patients.

Pagès et al[21] validated an immune score on the basis of the densities of $CD3^+$ and cytotoxic $CD8^+$ T cells in the tumor core and in the invasive margin for the prognostic classification of CRCs. They provided a reliable estimate of the risk of recurrence in patients with colon cancer, even for tumors with MSI features.

In this study, $CD3^+$ and $CD8^+$ T-cell subtype density by immunohistochemistry has shown to be higher in NOT COLD than in COLD tumors in both IM and CT, basically confirming the molecular results. Even if these differences do not reach statistical significance, probably depending on the limited number of analyzed samples, these results support the finding that the host antitumor immune response was most intense at IM, presumably to limit a further spread of malignant cells. These results are essentially in line with those recently reported by Yoon et al.[42] dMMR tumors are confirmed to have a significantly higher $CD3^+$ and $CD8^+$ T-cell subtype density compared with proficient MMR tumors; it is suggested that, at least in dMMR CRCs, the $CD3^+$ density within the infiltrative margin provided the most prognostic information.

It is clear that the presence of cytotoxic lymphocytes causes a compensatory up-regulation of suppressive immune elements directed to balance the immune system activity.[43] This could explain the dMMR tumor susceptibility to immunotherapies targeting suppressive immune checkpoints, especially PD-1 and PD-L1.[44] Recently, the efficacy of immune therapies has been demonstrated in dMMR tumors, although not all dMMR patients benefited from checkpoint inhibition.[45] Therefore, a further understanding of the immune microenvironment is necessary.

In this series, the PD-1 expression was observed in the tumoral cells in a few samples. On the other hand, PD-L1 was expressed in the tumoral cells of almost 50% of the analyzed samples and in a large majority of the sample lymphocytes. Interestingly, a high ratio of samples with PD-L1 expression in tumoral cells was observed in the samples with a HOT status of the immune system and with a high level of LyD (Figure 4, A and B). Instead, the ratio of PD-L1 positive tumoral cells was lower in the INTERMEDIATE and COLD samples and in the intermediate and lower LyD samples (Figure 4, B and C).

As to the future perspectives and implications of these results, their potential impact as predictive factors of immunotherapy efficacy should first be evaluated. Patients with NOT COLD tumors and in particular with HOT tumors (similar to inflamed tumors and characterized by an immunologically active tumor microenvironment) could benefit from a checkpoint inhibitor treatment (either in monotherapy or in association).[9–12] Vice versa, patients with COLD tumors (like noninflamed tumors and characterized by the absence of immune system activation) are unlikely to benefit from treatment with checkpoint inhibitors alone, but their sensitivity to immunotherapies can be restored through the association of chemotherapy and/or other systemic and locoregional treatments.[10] This could be verified by analyzing the immunoprofile expression of the samples of patients with metastatic CRC dMMR enrolled in phase 2 studies already completed with pembrolizumab and nivolumab.[3,5]

Finally, it could be useful to evaluate the application of the classifier also in patients with stable CRC, to select a group that can benefit from immunotherapy even among stable colorectal tumors. This classifier may be extended to other types of noncolorectal tumors to increase the cost/benefit ratio of immunotherapy. Despite the obvious need for further validation of these new findings, which should also include randomized trials, the potential selection of candidates for immunotherapy or other types of treatment appears to be extremely relevant and interesting.

Supplemental Data

Supplemental material for this article can be found at *https://doi.org/10.1016/j.jmoldx.2020.02.008*.

References

1. Gelsomino F, Barbolini M, Spallanzani A, Pugliese G, Cascinu S: The evolving role of microsatellite instability in colorectal cancer: a review. Cancer Treat Rev 2016, 51:19–26
2. Le DT, Durham JN, Smith KN, Wang H, Bartlett BR, Aulakh LK, et al: Mismatch repair deficiency predicts response of solid tumors to PD-1 blockade. Science 2017, 357:409–413
3. Le DT, Uram JN, Wang H, Bartlett BR, Kemberling H, Eyring AD, Skora AD, Luber BS, Azad NS, Laheru D, Biedrzycki B, Donehower RC, Zaheer A, Fisher GA, Crocenzi TS, Lee JJ, Duffy SM, Goldberg RM, de la Chapelle A, Koshiji M, Bhaijee F,

Huebner T, Hruban RH, Wood LD, Cuka N, Pardoll DM, Papadopoulos N, Kinzler KW, Zhou S, Cornish TC, Taube JM, Anders RA, Eshleman JR, Vogelstein B, Diaz LA: PD-1 blockade in tumors with mismatch-repair deficiency. N Engl J Med 2015, 372: 2509−2520

4. Overman MJ, Lonardi S, Wong KYM, Lenz H-J, Gelsomino F, Aglietta M, Morse MA, Van Cutsem E, McDermott R, Hill A, Sawyer MB, Hendlisz A, Neyns B, Svrcek M, Moss RA, Ledeine J-M, Cao ZA, Kamble S, Kopetz S, André T: Durable clinical benefit with nivolumab plus ipilimumab in DNA mismatch repair-deficient/microsatellite instability-high metastatic colorectal cancer. J Clin Oncol 2018, 36:773−779
5. Overman MJ, McDermott R, Leach JL, Lonardi S, Lenz H-J, Morse MA, Desai J, Hill A, Axelson M, Moss RA, Goldberg MV, Cao ZA, Ledeine J-M, Maglinte GA, Kopetz S, André T: Nivolumab in patients with metastatic DNA mismatch repair-deficient or microsatellite instability-high colorectal cancer (CheckMate 142): an open-label, multicentre, phase 2 study. Lancet Oncol 2017, 18: 1182−1191
6. Schreiber RD, Old LJ, Smyth MJ: Cancer immunoediting: integrating immunity's roles in cancer suppression and promotion. Science 2011, 331:1565−1570
7. Dunn GP, Old LJ, Schreiber RD: The immunobiology of cancer immunosurveillance and immunoediting. Immunity 2004, 21: 137−148
8. Vesely MD, Kershaw MH, Schreiber RD, Smyth MJ: Natural innate and adaptive immunity to cancer. Annu Rev Immunol 2011, 29: 235−271
9. Trujillo JA, Sweis RF, Bao R, Luke JJ: T cell-inflamed versus non-T cell-inflamed tumors: a conceptual framework for cancer immunotherapy drug development and combination therapy selection. Cancer Immunol Res 2018, 6:990−1000
10. Boland PM, Ma WW: Immunotherapy for colorectal cancer. Cancers 2017, 9:E50
11. Spranger S, Luke JJ, Bao R, Zha Y, Hernandez KM, Li Y, Gajewski AP, Andrade J, Gajewski TF: Density of immunogenic antigens does not explain the presence or absence of the T-cell-inflamed tumor microenvironment in melanoma. Proc Natl Acad Sci U S A 2016, 113:E7759−E7768
12. Gajewski TF, Corrales L, Williams J, Horton B, Sivan A, Spranger S: Cancer immunotherapy targets based on understanding the T cell-inflamed versus non-T cell-inflamed tumor microenvironment. Adv Exp Med Biol 2017, 1036:19−31
13. Fridman WH, Pagès F, Sautès-Fridman C, Galon J: The immune contexture in human tumours: impact on clinical outcome. Nat Rev Cancer 2012, 12:298−306
14. Melero I, Rouzaut A, Motz GT, Coukos G: T-cell and NK-cell infiltration into solid tumors: a key limiting factor for efficacious cancer immunotherapy. Cancer Discov 2014, 4:522−526
15. Bindea G, Mlecnik B, Tosolini M, Kirilovsky A, Waldner M, Obenauf AC, Angell H, Fredriksen T, Lafontaine L, Berger A, Bruneval P, Fridman WH, Becker C, Pagès F, Speicher MR, Trajanoski Z, Galon J: Spatiotemporal dynamics of intratumoral immune cells reveal the immune landscape in human cancer. Immunity 2013, 39:782−795
16. Newman AM, Liu CL, Green MR, Gentles AJ, Feng W, Xu Y, Hoang CD, Diehn M, Alizadeh AA: Robust enumeration of cell subsets from tissue expression profiles. Nat Methods 2015, 12: 453−457
17. Szklarczyk D, Morris JH, Cook H, Kuhn M, Wyder S, Simonovic M, Santos A, Doncheva NT, Roth A, Bork P, Jensen LJ, von Mering C: The STRING database in 2017: quality-controlled protein−protein association networks, made broadly accessible. Nucleic Acids Res 2017, 45:D362−D368
18. Enright AJ, Van Dongen S, Ouzounis CA: An efficient algorithm for large-scale detection of protein families. Nucleic Acids Res 2002, 30: 1575−1584
19. Goswami S, Chakrabarti A: Quartile clustering: a quartile based technique for generating meaningful clusters. J Comput 2012, 4: 48−55
20. Janowitz MF, Schweizer B: Ordinal and percentile clustering. Math Soc Sci 1989, 18:135−186
21. Pagès F, Mlecnik B, Marliot F, Bindea G, Ou F-S, Bifulco C, et al: International validation of the consensus immunoscore for the classification of colon cancer: a prognostic and accuracy study. Lancet 2018, 391:2128−2139
22. Berntsson J, Eberhard J, Nodin B, Leandersson K, Larsson AH, Jirström K: Expression of programmed cell death protein 1 (PD-1) and its ligand PD-L1 in colorectal cancer: relationship with sidedness and prognosis. Oncoimmunology 2018, 7:e1465165
23. Mekenkamp LJM, Koopman M, Teerenstra S, van Krieken JHJM, Mol L, Nagtegaal ID, Punt CJA: Clinicopathological features and outcome in advanced colorectal cancer patients with synchronous vs metachronous metastases. Br J Cancer 2010, 103:159−164
24. Deschoolmeester V, Baay M, Van Marck E, Weyler J, Vermeulen P, Lardon F, Vermorken JB: Tumor infiltrating lymphocytes: an intriguing player in the survival of colorectal cancer patients. BMC Immunol 2010, 11:19
25. Boissière-Michot F, Lazennec G, Frugier H, Jarlier M, Roca L, Duffour J, Du Paty E, Laune D, Blanchard F, Le Pessot F, Sabourin J-C, Bibeau F: Characterization of an adaptive immune response in microsatellite-instable colorectal cancer. Oncoimmunology 2014, 3: e29256
26. Maby P, Tougeron D, Hamieh M, Mlecnik B, Kora H, Bindea G, Angell HK, Fredriksen T, Elie N, Fauquembergue E, Drouet A, Leprince J, Benichou J, Mauillon J, Le Pessot F, Sesboüé R, Tuech J-J, Sabourin J-C, Michel P, Frébourg T, Galon J, Latouche J-B: Correlation between density of CD8+ T-cell infiltrate in microsatellite unstable colorectal cancers and frameshift mutations: a rationale for personalized immunotherapy. Cancer Res 2015, 75:3446−3455
27. Hutchins G, Southward K, Handley K, Magill L, Beaumont C, Stahlschmidt J, Richman S, Chambers P, Seymour M, Kerr D, Gray R, Quirke P: Value of mismatch repair, KRAS, and BRAF mutations in predicting recurrence and benefits from chemotherapy in colorectal cancer. J Clin Oncol 2011, 29:1261−1270
28. Roth AD, Tejpar S, Delorenzi M, Yan P, Fiocca R, Klingbiel D, Dietrich D, Biesmans B, Bodoky G, Barone C, Aranda E, Nordlinger B, Cisar L, Labianca R, Cunningham D, Van Cutsem E, Bosman F: Prognostic role of KRAS and BRAF in stage II and III resected colon cancer: results of the translational study on the PETACC-3, EORTC 40993, SAKK 60-00 trial. J Clin Oncol 2010, 28:466−474
29. Giannini R, Ugolini C, Poma AM, Urpì M, Niccoli C, Elisei R, Chiarugi M, Vitti P, Miccoli P, Basolo F: Identification of two distinct molecular subtypes of non-invasive follicular neoplasm with papillary-like nuclear features by digital RNA counting. Thyroid 2017, 27:1267−1276
30. Bruno R, Alì G, Giannini R, Proietti A, Lucchi M, Chella A, Melfi F, Mussi A, Fontanini G: Malignant pleural mesothelioma and mesothelial hyperplasia: a new molecular tool for the differential diagnosis. Oncotarget 2017, 8:2758−2770
31. Hagerling C, Casbon A-J, Werb Z: Balancing the innate immune system in tumor development. Trends Cell Biol 2015, 25: 214−220
32. Marty Pyke R, Thompson WK, Salem RM, Font-Burgada J, Zanetti M, Carter H: Evolutionary pressure against MHC class II binding cancer mutations. Cell 2018, 175:1991
33. Haabeth OAW, Fauskanger M, Manzke M, Lundin KU, Corthay A, Bogen B, Tveita AA: CD4+ T-cell-mediated rejection of MHC class II-positive tumor cells is dependent on antigen secretion and indirect presentation on host APCs. Cancer Res 2018, 78:4573−4585
34. Nair S, Dhodapkar MV: Natural killer T cells in cancer immunotherapy. Front Immunol 2017, 8:1178

35. Coppola A, Arriga R, Lauro D, Del Principe MI, Buccisano F, Maurillo L, Palomba P, Venditti A, Sconocchia G: NK cell inflammation in the clinical outcome of colorectal carcinoma. Front Med (Lausanne) 2015, 2:33
36. Rocca YS, Roberti MP, Juliá EP, Pampena MB, Bruno L, Rivero S, Huertas E, Sánchez Loria F, Pairola A, Caignard A, Mordoh J, Levy EM: Phenotypic and functional dysregulated blood NK cells in colorectal cancer patients can be activated by cetuximab plus IL-2 or IL-15. Front Immunol 2016, 7:413
37. Cantoni C, Huergo-Zapico L, Parodi M, Pedrazzi M, Mingari MC, Moretta A, Sparatore B, Gonzalez S, Olive D, Bottino C, Castriconi R, Vitale M: NK cells, tumor cell transition, and tumor progression in solid malignancies: new hints for NK-based immunotherapy? J Immunol Res 2016, 2016:4684268
38. Susek KH, Karvouni M, Alici E, Lundqvist A: The role of CXC chemokine receptors 1-4 on immune cells in the tumor microenvironment. Front Immunol 2018, 9:2159
39. Xu Y, Xu Q, Ni S, Liu F, Cai G, Wu F, Ye X, Meng X, Mougin B, Cai S, Du X: Decrease in natural killer cell associated gene expression as a major characteristic of the immune status in the bloodstream of colorectal cancer patients. Cancer Biol Ther 2011, 11:188−195
40. Saito T, Nishikawa H, Wada H, Nagano Y, Sugiyama D, Atarashi K, Maeda Y, Hamaguchi M, Ohkura N, Sato E, Nagase H, Nishimura J, Yamamoto H, Takiguchi S, Tanoue T, Suda W, Morita H, Hattori M, Honda K, Mori M, Doki Y, Sakaguchi S: Two FOXP3(+)CD4(+) T cell subpopulations distinctly control the prognosis of colorectal cancers. Nat Med 2016, 22:679−684
41. Roelands J, Kuppen PJK, Vermeulen L, Maccalli C, Decock J, Wang E, Marincola FM, Bedognetti D, Hendrickx W: Immunogenomic classification of colorectal cancer and therapeutic implications. Int J Mol Sci 2017, 18:2229
42. Yoon HH, Shi Q, Heying EN, Muranyi A, Bredno J, Ough F, Djalilvand A, Clements J, Bowermaster R, Liu W-W, Barnes M, Alberts SR, Shanmugam K, Sinicrope FA: Intertumoral heterogeneity of CD3+ and CD8+ T-cell densities in the microenvironment of DNA mismatch-repair−deficient colon cancers: implications for prognosis. Clin Cancer Res 2019, 25:125−133
43. de Vries NL, Swets M, Vahrmeijer AL, Hokland M, Kuppen PJK: The immunogenicity of colorectal cancer in relation to tumor development and treatment. Int J Mol Sci 2016, 17:1030
44. Quiroga D, Lyerly HK, Morse MA: Deficient mismatch repair and the role of immunotherapy in metastatic colorectal cancer. Curr Treat Options Oncol 2016, 17:41
45. Kalyan A, Kircher S, Shah H, Mulcahy M, Benson A: Updates on immunotherapy for colorectal cancer. J Gastrointest Oncol 2018, 9:160−169